

Simple model of excitable media with dispersion and curvature

Hiroyuki Ito*

Department of Physiology, McGill University, 3655 Drummond Street, Montreal, Quebec, Canada H3G 1Y6

(Received 2 March 1992)

An alternative theoretical model that incorporates the experimentally measurable dispersion relation is used to study the curvature effect and the dynamics of spiral waves in two-dimensional excitable media. The model is constructed to abstract the most significant factors leading to phenomena observed universally in excitable media. The analytically derived curvature relation and critical radius show an excellent agreement with numerical simulations of the model. Both stationary rotating spirals and a meandering motion are observed numerically, in accord with other experimental and theoretical studies.

PACS number(s): 82.20.Wt, 82.20.Mj, 87.10.+e

Spiral waves of excitation are observed in a wide variety of excitable media and their dynamical behaviors have attracted much attention for many years [1]. Traditionally theoretical studies have been carried out mainly by using nonlinear partial differential equations (PDE's) [2,3]. Quite recently, however, cellular-automaton models with multiple states [4–6] and coupled-map lattices [7] have been proposed for faster numerical computations. All of these models are based on the *microscopic* physical mechanism of generation and propagation of excitation and are used to simulate spiral waves observed at a *macroscopic* level. Due to the complexity of their mathematical structure, analytical studies are difficult and most studies are carried out by computer simulations except for some studies of perturbation analysis [3,8]. A difficulty has been pointed out [9] also in quantitative comparison of the results of PDE's with the experimental data, because some of the important parameters remain poorly measured. The disagreement of the dispersion relation computed by the Oregonator model with the experimental data of the Belousov-Zhabotinskii (BZ) reaction was attributed to discrepancies in quantitative comparison of spiral waves [9,5].

In this Brief Report, we introduce an alternative theoretical model from a different point of view. Since spiral waves are observed universally, there should exist some universal characteristics between the microscopic level and the macroscopic level of general excitable media. The motivation of our modeling is to provide a tool that is used to abstract these most essential factors determining the characteristics of spiral waves. The importance of such an approach has been pointed out by Zykov [10] in his kinematic approach. We construct our model based on the essential characteristic in a “mesoscopic” level of excitable media (*dispersion relation*): the propagation velocity of excitation wave front depends on the *recovery time*, that is, the time elapsed since the passage of the last excitation [11]. Since the dispersion relation can be easily measured experimentally, we can explicitly incorporate these data into the model to study the spiral waves and can compare the quantitative results directly with the experimental data. The simple mathematical structure of the model enables us to derive the exact nonlinear curvature relation. In the previous

studies by PDE's, the curvature relation has been calculated only by a perturbation method in the limit of some small parameter.

The solid line in Fig. 1(a) shows the dispersion relation of the plane wave in the BZ reaction, $c_{BZ}(T)$, obtained by a least-square fitting of experimental data [12] assuming the functional form.

$$c(T) = 1/[\alpha \exp(-T/\beta) + \gamma] \quad \text{if } T \geq \theta, \quad (1)$$

where α , β , and γ are positive parameters and T is the recovery time. After the excitation, the media needs a certain time interval, called the *refractory period* θ , to re-

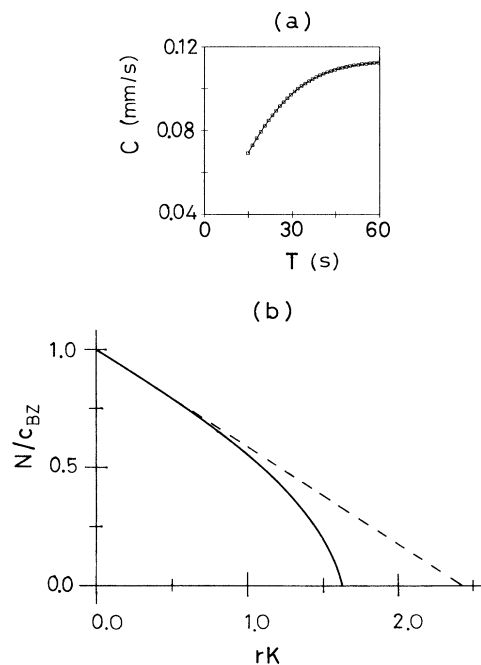


FIG. 1. (a) Dispersion relation: fitted curve based on data of the BZ reaction (solid line) and the numerical simulation of the model (open squares). (b) Curvature relation: normal velocity of curved front $N(K, T)$ scaled by the velocity of plane wave $c_{BZ}(T)$ is plotted as a function of the scaled curvature rK (solid line). The linear relation (dashed line) approximates N in the region of small K .

cover its ability to conduct excitation. The fitted parameters are $\alpha_{\text{BZ}}=21.7$ s/mm, $\beta_{\text{BZ}}=11.1$ s, and $\gamma_{\text{BZ}}=8.79$ s/mm, and we estimate $\theta_{\text{BZ}}=15$ s from the experimental data. This relation reflects slow conduction velocity for short recovery time due to incomplete recovery of excitability of media.

At first we consider a regular square lattice of $N \times N$ excitable elements (cells) with identical property with a lattice constant d . The term ‘‘cell’’ is used here in a technical sense and does not correspond to a biological cell. Each cell is connected to all the neighboring cells within a circle of an interaction radius r by a conducting cable. The cell can be excited by incoming pulses from exciting neighboring cells. When a cell gets excited, it emits an excitation pulse which conducts to its neighboring cells through the conducting cable. We assume that the conduction velocity of the pulse v depends on the recovery time T , that is, the time interval from the preceding excitation to the present excitation at the cell which is emitting the pulses. The cell gets excited when a sequence of pulses exceeding a finite threshold number N_{th} arrive after the refractory duration with a high frequency so that all the pulses arrive within a finite time interval t_w . The next excitation will be induced at the instant when N_{th} th pulse arrives at the cell. The cell is more excitable with smaller N_{th} and larger t_w .

A single cell needs to wait for many incoming pulses to propagate the excitation wave and this leads to a conduction delay of the wave front. Therefore the propagation velocity of the macroscopic wave front is smaller than the local conduction velocity of pulses between the neighboring cells. At first local conduction velocity of excitation pulses $v(T)$ should be determined so that the plane wave satisfies the dispersion relation of the BZ reaction $c_{\text{BZ}}(T)$. The continuum limit of the model can be taken when the lattice constant d goes to zero, keeping the total size $L=Nd, r, t_w$, and the ratio $p=N_{\text{th}}/\mathcal{N}_{\text{NN}}$ constant, where \mathcal{N}_{NN} is the number of neighboring cells within the interaction range [$\pi(r/d)^2$ in the continuum limit]. We consider the propagation of plane wave with a constant velocity in the continuum limit and calculate the domain of neighbors that contributes to the excitation of the cell. A simple computation can lead to a relation [13]

$$v(T) = c_{\text{BZ}}(T) / \cos(p\pi). \quad (2)$$

Therefore $v(T)$ should obey the relation (1) with the parameters $\alpha = \cos(p\pi)\alpha_{\text{BZ}}$, $\beta = \beta_{\text{BZ}}$, $\gamma = \cos(p\pi)\gamma_{\text{BZ}}$, and $\theta = \theta_{\text{BZ}}$ to realize the dispersion relation $c_{\text{BZ}}(T)$. It must be noted that by using the relation (2), the model can be adjusted to realize any given dispersion relation. We consider that only the property in the continuum limit of the model is physically relevant. A finite lattice constant d and a dynamical element ‘‘cell’’ are introduced simply to facilitate numerical simulations and d should be small enough so that the results do not depend on its value. Therefore our model is essentially a continuum model both spatially and temporally.

We confirmed the dispersion relation by numerical simulations of the model. The periodic boundary condition is imposed on both opposite sides of the lattice of

$20 \times N_y$ cells (i.e., torus shape). We initiate a unidirectional circulation of plane wave along the y direction and calculate the steady-state circulation period T_0 after the initial transient dies out. By changing N_y , we get the relation between the recovery time T_0 and the propagation velocity of plane wave $c_S = L_y/T_0$, where $L_y = N_y d$. In actual numerical simulations, to better reproduce the results in the continuum limit using the system with a finite d , we randomize the position of the cells [6]. The position of each cell deviates randomly from its regular position by δx in the x direction (δy in the y direction), where both δx and δy are independently Gaussian distributed with mean zero and standard deviation σ . The open squares in Fig. 1(a) show the results with $r=0.1$ mm, $d=r/6$, $N_{\text{th}}=42$, and $\sigma=0.3d$ [$\mathcal{N}_{\text{NN}} = \pi(r/d)^2 \sim 113.1$]. The center of the open square is the average over ten samples with different random distributions of cells. The data show an excellent agreement with the dispersion curve and the statistical error is barely visible.

In two dimensions, the curved wave front propagates with a velocity that depends on its curvature. The curvature relation is another important ‘‘mesoscopic’’ characteristic other than the dispersion relation [2,3]. The normal propagation velocity $N(K, T)$ of the curved convex wave front with a curvature $K (>0)$ can be derived analytically in a similar way as the dispersion relation. $N(K, T)$ is expressed by a nonlinear function using the root of a transcendental equation [13]. Figure 1(b) shows $N(K, T)$ obtained by solving the transcendental equation numerically with $p=0.3118$. In general $N(K, T)$ is a concave-down function of K ending at K_{cr} taking $N=0$. The critical curvature K_{cr} above which the curved wave front fails to propagate can be calculated by the root of another transcendental equation $N(K_{\text{cr}}, T)=0$ [13]. A perturbation expansion in case of small curvature leads to a familiar linear curvature relation,

$$N(K, T) \sim c_{\text{BZ}}(T) - D(T)K, \quad K \ll 1/r, \quad (3)$$

where $D(T) = [\sin^2 p\pi / (3 \cos p\pi)] r c_{\text{BZ}}(T)$ and corresponds to the ‘‘diffusion coefficient’’ of the media when we compare Eq. (3) with the linear curvature relation of PDE’s [2,3,14]. The solid line in Fig. 2(a) shows the dependence of the critical radius $R_{\text{cr}} = 1/K_{\text{cr}}$ on the parameter p in a range $0.25 < p < 0.5$. The critical radius obtained by assuming the linear curvature relation in Eq. (3), $D(T)/c_{\text{BZ}}(T) = [\sin^2 p\pi / (3 \cos p\pi)] r$, is plotted by a dashed line. As known from Fig. 2(a), the nonlinear function $N(K, T)$ is well approximated by the linear function in Eq. (3) when p is close to 0.5.

The critical radius R_{cr} can be confirmed by numerical simulations. At $t=0$, all cells within a circle of radius R_{stim} at the center of the system are excited. The critical radius R_{cr} is the smallest value of R_{stim} that leads to an outward propagation of the circular wave. In this simulation, each cell is fully recovered before its excitation. The critical radius averaged over 30 samples with different random distributions is plotted in Fig. 2(a) ($r=0.1$ mm, $d=r/6$, $\sigma=0.3d$, $30 \leq N_{\text{th}} \leq 49$). The data shows a fairly good agreement with the theoretical value by the nonlinear curvature relation. The ‘‘diffusion

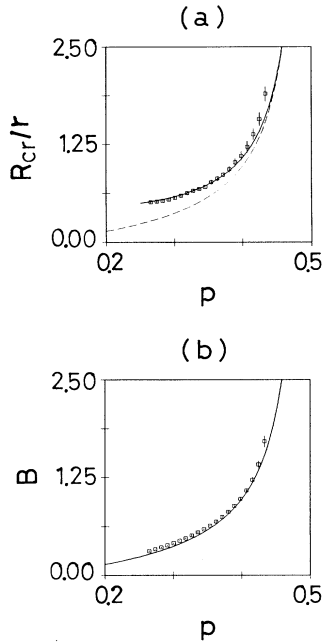


FIG. 2. Dependence of various quantities on p . (a) Critical radius R_{cr} scaled by r : theoretical curve by the nonlinear curvature relation (solid line), by the linear curvature relation (dashed line), and the numerical simulations (open squares). (b) Scaled diffusion coefficient B : theoretical curve (solid line) and the numerical simulations (open squares).

coefficient" in the linear curvature relation in Eq. (3) was also checked by numerical simulations. The circular wave is initiated at $t=0$ by the same method and the distance from the center and the time of excitation is measured for each cell. The relation between the two quantities is well fitted by the theoretical curve obtained by assuming Eq. (3). Figure 2(b) plots the quantity $B = \bar{D}/(r\bar{c}_{BZ})$ averaged over 30 samples, where \bar{D} and \bar{c}_{BZ} are the fitted parameters. The numerical data shows a good agreement with the theoretical value of $B = \sin^2 p \pi / (3 \cos p \pi)$ [solid line in Fig. 2(b)].

In the previous discussion, the nature of the wave propagation was not influenced by the time interval t_w as long as t_w is not too small. However, the property of spiral waves strongly depends on t_w because spiral wave adjusts its geometry (rotation period and core size) depending on the excitability of media. With the parameters $r=0.1$ mm, $d=r/6$, $N_{th}=42$, and $\sigma=0.3d$, the system of 100×100 cells supports a stationary rotating spiral wave with constant rotation period T_0 over a wide range of t_w (2.0 s $\leq t_w \leq 6.0$ s) that we have examined [15]. Figure 3(a) shows the excited cells during a time interval of 1 s accompanied by the counterclockwise revolution of spiral wave ($t_w=4.0$ s and $T_0=23.1$ s). The successive excited regions separated by 3.6 s are overwritten to animate the revolution of the spiral. We take open boundary condition, that is, the cells on the boundary are connected to the inside cells only. Around the center of the spiral, there exists a self-organized circular core region in which cells cannot be excited because the high curvature of the tip of the spiral wave prevents these cells

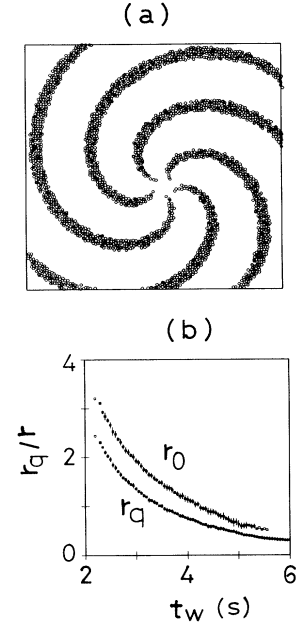


FIG. 3. (a) Stationary rotating spiral wave. Each region shows the successive excitation of cells separated by 3.6 s. The size of the system is 1.67×1.67 mm². (b) Dependence of the core radius r_q (scaled by r) on t_w . The core radius r_0 by the Tyson-Keener formula is also plotted.

from receiving more than N_{th} pulses within t_w . We measured the steady rotation period T_0 and the core radius $r_q = (\mathcal{N}_q/\pi)^{1/2}d$, after spiral rotation becomes stationary. \mathcal{N}_q is the sum of the number of cells forming the core and that of cells on the tip trace surrounding the core [16]. Figure 3(b) shows r_q as a function of t_w . Each point is the average over many samples (10–30). T_0 is also a monotonically decreasing function of t_w with a finite asymptote (figure not shown). Tyson and Keener [3] have derived an approximate formula for the relation between T_0 and the core radius r_0 . This relation is universal for any excitable media described by the general reaction diffusion equations. r_0 is the radius where the spiral wave front has zero tangential velocity; its relation to r_q is still unclear except that r_0 is a little larger than r_q . We calculate r_0 from T_0 by applying their formula and plot in Fig. 3(b). Our results for spiral waves is consistent with the result of PDE's.

The simulations in Figs. 3(a)–3(b) were carried out with the "diffusion coefficient" $D = (6-7) \times 10^{-3}$ mm²/s that is larger than the value of the BZ reaction ($D_{BZ} = 2 \times 10^{-3}$ mm²/s). The model has three parameters r , p , and t_w that should be determined to realize the spiral wave in the BZ reaction. By using $T_0 \sim 17.3$ s [12], we determine $r = 0.06024$ mm and $p = 0.3183$ ($N_{th} = 36$) to realize D_{BZ} [17]. However, in the numerical simulations with these parameters, we do not obtain a stationary rotating spiral wave over a range of 1.5 s $\leq t_w \leq 6.0$ s that we have examined. The tip traces a flower-petal pattern as shown in Fig. 4 ($t_w = 1.5$ s) and the trace does not close. Such a meandering motion has been widely observed both experimentally [9,18] and numerically

[9,19,7]. With $t_w = 1.7$ s, the mean rotation period of the meandering spiral \bar{T}_0 is about 17.3 s, that is, close to the rotation period of the stationary spiral in the BZ reaction. The meander of the tip is confined to a region of radius $r_{\text{eff}} \sim 0.13$ mm. This amount is close to the theoretical estimation by the Tyson-Keener formula ($r_0 = 0.12$ mm) and the core size in the BZ reaction (0.09 mm) [20,5]. By numerical simulations using the Oregonator model, Tyson and Keener [3] were also unsuccessful in obtaining a stationary spiral. However our result shows a better quantitative agreement with experimental data than their data of meandering spiral ($r_{\text{eff}} = 0.18$ mm and $\bar{T}_0 = 20$ s).

In summary, we introduce a simple model of excitable media based only on “mesoscopic” characteristics of the media (dispersion relation and curvature relation). The model successfully reproduces the dynamical behavior observed universally in excitable media (stationary spiral with a core and meandering) in accord with other experimental and theoretical studies. Therefore we demonstrate that dispersion relation and curvature relation are the most significant factors determining the characteristics of spiral waves. Since these relations are easily measurable in experiment, the model provides more interactive connection between experiment and theory than the previous theoretical models.

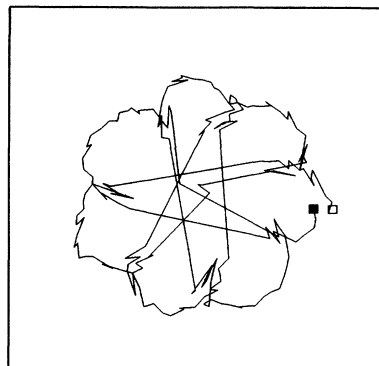


FIG. 4. Trace of the tip of meandering spiral over 73 s. The tip starts from the open square and ends at the closed square. The size of the box is 0.75×0.75 mm².

The author thanks L. Glass, A. T. Winfree, M. Courtemanche, and D. Kaplan for valuable discussions. This research was supported by grants from the Natural Science and Engineering Research Council of Canada and les Fonds des Recherches en Santé du Québec. The author was supported by the Heart and Stroke Foundation of Canada.

*Present address: Department of Information Science and Communication, Kyoto Sangyo University, Kamigamo, Kita-ku, Kyoto 603, Japan.

- [1] A. T. Winfree, *When Time Breaks Down* (Princeton University Press, Princeton, 1987).
- [2] V. S. Zykov, *Simulation of Wave Processes in Excitable Media* (Manchester University Press, Manchester, 1987).
- [3] J. J. Tyson and J. P. Keener, *Physica D* **32**, 327 (1988).
- [4] M. Gerhardt, H. Schuster, and J. J. Tyson, *Science* **247**, 1563 (1990).
- [5] M. Gerhardt, H. Schuster, and J. J. Tyson, *Physica D* **46**, 392 (1990); *ibid.* 416.
- [6] M. Markus and B. Hess, *Nature* **347**, 56 (1990).
- [7] D. Barkley, M. Kness, and L. S. Tuckerman, *Phys. Rev. A* **42**, 2489 (1990).
- [8] P. Pelce and J. Sun, *Physica D* **48**, 353 (1991); A. Karma, *Phys. Rev. Lett.* **68**, 397 (1992); D. A. Kessler, H. Levine, and W. N. Reynolds, *ibid.* **68**, 401 (1992).
- [9] W. Jahnke, W. E. Skaggs, and A. T. Winfree, *J. Phys. Chem.* **93**, 740 (1989).
- [10] V. S. Zykov, *Biophysics* **32**, 365 (1987).
- [11] The simplest model with only nearest-neighbor couplings has been applied to study breakup of spiral waves and reentrant excitation in a ring of cardiac tissue: H. Ito and L. Glass, *Phys. Rev. Lett.* **66**, 671 (1991); *Physica D* **56**, 84 (1992). However, since discreteness is very essential in this model and this does not show any curvature relation, the present model is significantly different from this model.
- [12] P. Foerster, S. C. Müller, and B. Hess, *Proc. Natl. Acad. Sci. USA* **86**, 6831 (1989).
- [13] The details of these calculations will be presented in a full length paper.
- [14] In our model, D is proportional to $c_{\text{BZ}}(T)$, because the excitation spreads out by conduction of excitation pulses, that is, interaction is of convolution type. This is not the case for PDE's, in which the excitation spreads out by a molecular diffusion. In a PDE of two components, D is proved to be equal to the diffusion coefficient and be constant only when both components have the same diffusion coefficient or when the diffusion coefficient of the inhibitor is zero and the smallness parameter ϵ goes to zero. It is a very important problem whether the slope of the linear curvature relation in actual media depends on T or not. However, there has been no systematic report on this yet [A. T. Winfree (private communication)].
- [15] In the numerical simulations, the simply rotating spiral solution may coexist with the other spiral solution whose tip travels the closed noncircular line. This might be related with mode-locked meandering motion. In Fig. 3(b), we averaged the data only over the samples of stationary spirals.
- [16] The position of the tip is determined by the cell that has a nonexcited nearest-neighbor cell during a reasonably long time interval around its own excitation.
- [17] Since D depends on both r and p , it is impossible to determine the unique set of (r, p) based only on the linear curvature relation. The difference appears only in the region of a large curvature where the nonlinearity in $N(K)$ is dominant. We chose them for numerical convenience.
- [18] G. S. Skinner and H. L. Swinney, *Physica D* **48**, 1 (1991).
- [19] E. Lugosi, *Physica D* **40**, 331 (1989).
- [20] S. C. Müller, T. Plesser, and B. Hess, *Science* **230**, 661 (1985).